hep-ex/9907005 7 Jul 1999

FIRST OBSERVATION OF THE $\phi \to \pi^+\pi^-\gamma$ DECAY

R.R.Akhmetshin, E.V.Anashkin, M.Arpagaus, V.M.Aulchenko, V.S.Banzarov, L.M.Barkov, N.S.Bashtovoy, A.E.Bondar, D.V.Bondarev, A.V.Bragin, D.V.Chernyak, A.S.Dvoretsky, S.I.Eidelman, G.V.Fedotovich, N.I.Gabyshev, A.A.Grebeniuk, D.N.Grigoriev, P.M.Ivanov, S.V.Karpov, V.F.Kazanin, B.I.Khazin, I.A.Koop, P.P.Krokovny, L.M.Kurdadze, A.S.Kuzmin, I.B.Logashenko, P.A.Lukin, A.P.Lysenko, K.Yu.Mikhailov, I.N.Nesterenko, V.S.Okhapkin, E.A.Perevedentsev, E.A.Panich, A.S.Popov, T.A.Purlatz, N.I.Root, A.A.Ruban, N.M.Ryskulov, A.G.Shamov, Yu.M.Shatunov, B.A.Shwartz, A.L.Sibidanov, V.A.Sidorov, A.N.Skrinsky, V.P.Smakhtin, I.G.Snopkov, E.P.Solodov, P.Yu.Stepanov, A.I.Sukhanov, V.M.Titov, Yu.V.Yudin, S.G.Zverev
Budker Institute of Nuclear Physics, Novosibirsk, 630090, Russia

J.A.Thompson
University of Pittsburgh, Pittsburgh, PA 15260, USA

Abstract

Radiative decays of the ϕ meson have been studied using a data sample of about 20 million ϕ decays collected by the CMD-2 detector at VEPP-2M collider in Novosibirsk. From selected $e^+e^- \to \pi^+\pi^-\gamma$ events the $\phi \to \pi^+\pi^-\gamma$ decay has been observed for the first time.

Under the assumption that the intermediate $f_0(980)\gamma$ state dominates in the $\phi \to \pi^+\pi^-\gamma$ decay, the corresponding branching ratio is $Br(\phi \to f_0(980)\gamma) = (1.93 \pm 0.46 \pm 0.50) \times 10^{-4}$.

Selected $e^+e^- \to \mu^+\mu^-\gamma$ events were used to obtain $Br(\phi \to \mu^+\mu^-\gamma) = (1.43 \pm 0.45 \pm 0.14) \times 10^{-5}$ for $E_\gamma > 20$ MeV.

Using the same data sample, upper limits at 90% CL have been obtained for the C-violating decay of the ϕ: $Br(\phi \to \rho\gamma) < 1.2 \times 10^{-5}$; and for the P- and CP-violating decay of the η:
$Br(\eta \to \pi^+\pi^-) < 3.3 \times 10^{-4}$.

Introduction

The identification of scalar mesons and particularly the determination of the lightest scalar $q\bar{q}$ nonet is of extreme importance both for quark systematics and searches for non-$q\bar{q}$ objects like glueballs and multiquark states (see the discussion of this problem in the minireview on scalar mesons by S.Spanier and N.Törnqvist, p.390 of Ref. [1]). It is generally accepted that the probabilities of the electric dipole radiative transitions of the ϕ meson are crucial for the clarification of the nature of $f_0(980)$ and $a_0(980)$ mesons [2, 3]. A search for these decays has been earlier performed by the ND [4] and CMD-2 [5] groups. A number of new results has been recently published by SND [

6, 7] and CMD-2 [8, 9] collaborations at the e^+e^- collider VEPP-2M [10] where the radiative decays $\phi \to \pi^0\pi^0\gamma$, $\phi \to \eta\pi^0\gamma$ and $\phi \to \pi^+\pi^-\gamma$ have been observed for the first time.

The mode with two charged pions has very large background because of the radiative processes $e^+e^- \to \pi^+\pi^-\gamma$ where a photon comes from initial electrons or from final pions. Therefore a signal from the $f_0(980)\gamma$ final state can be seen as an interference structure at the energy $E_\gamma = \frac{m_\phi^2 - m_{f_0^2}}{2m_\phi} \approx 40$ MeV in the photon spectrum. The shape of this structure depends on the $f_0(980)$ mass and width. In our first paper [5] a search for the $\phi \to \pi^+\pi^-\gamma$ decay led to the upper limit of 3×10^{-5} that looked at first puzzlingly low compared to the decay $\phi \to \pi^0\pi^0\gamma$ observed with the branching ratio of about 1×10^{-4} [7]. As was shown in [8, 5, 11], in case of the $\phi \to f_0(980)\gamma$ intermediate state it could be explained by the destructive interference between bremsstrahlung processes and the ϕ decay.

In this paper results of the study of the $e^+e^- \to \pi^+\pi^-\gamma$ process with the CMD-2 detector [12] are presented. In total, the 14.2 pb^{-1} of data have been collected since 1993 at 14 energy points around the ϕ mass. For the analysis of the $\pi^+\pi^-\gamma$ decay mode 13.1 pb^{-1} corresponding to 19.7×10^6 ϕ decays were used. Seven scans of this energy region were performed allowing control of systematic errors caused by possible detector instability. The results obtained from individual scans were found to be consistent.

Selection of $\pi^+\pi^-\gamma$ Events

Event candidates were selected by requiring only two minimum ionizing tracks in the drift chamber (DC) and one or two photons with energy greater than 20 MeV in the CsI calorimeter. The following selection criteria were used:

1. The average momentum of two charged particles is higher than 240 MeV/c to remove the background from $K_S \to \pi^+\pi^-$ decays.

2. Detected tracks have a polar angle between 1.05 and 2.1 radians so that they enter the inner muon system.

3. The sum of the energy depositions of two clusters associated with two tracks is less than 450 MeV to remove Bhabha events.

4. The radial distance of the closest approach of each track to the beam axis is less than 0.3 cm.

5. The Z-coordinate of the vertex (along the beam) is within 10 cm from the detector center. This cut reduces cosmic ray background by a factor of two.

6. Detected photons have a polar angle between 0.85 and 2.25 radians so that they enter the "good" region in the CsI barrel calorimeter. This requirement suppressed the background from the photons emitted by initial electrons.

7. Events with an invariant mass of two photons close to the π^0 mass ($|m_{\gamma\gamma} - m_{\pi^0}| < 40$ MeV) were removed.

After the above cuts the main background for the $\pi^+\pi^-\gamma$ final state comes from: a) the radiative process $e^+e^- \to \mu^+\mu^-\gamma$, b) the decay $\phi \to \pi^+\pi^-\pi^0$ when one of the photons from the π^0 escapes detection and c) collinear events $e^+e^- \to \mu^+\mu^-, \pi^+\pi^-$ in which secondary decays and interactions of muons or pions with the detector material produce a background cluster mimicking a photon.

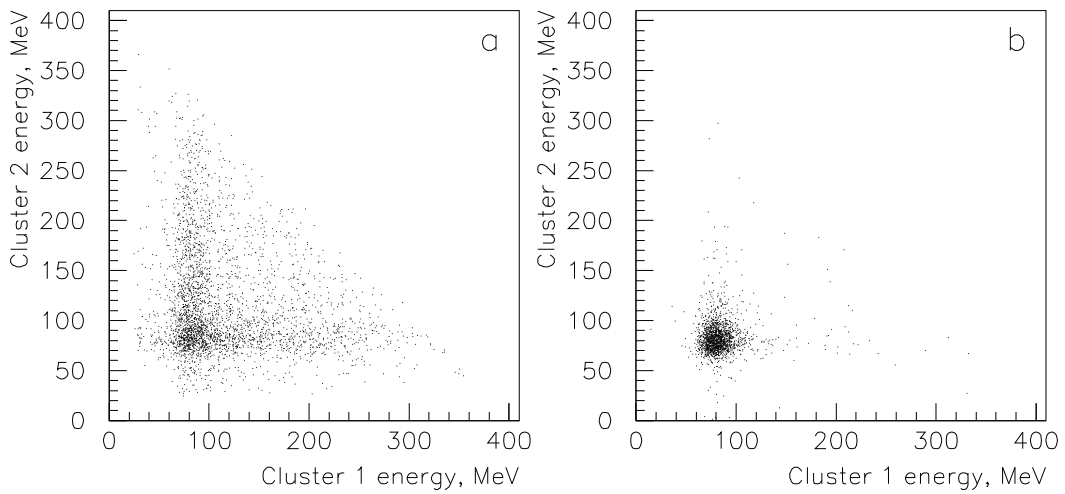

Figure 1: Calorimeter response for events with one or no hits in the muon system (a) and for events selected as muons (b).

Selection of $\mu^+\mu^-\gamma$ Events

The inner muon system was used to separate muons from pions. The muon system uses streamer tubes grouped in two layers (inner and outer) with a 15 cm magnet yoke serving as an absorber and has 1-3 cm spatial resolution. The requirement of hits in the inner muon system for both charged particles selects muon events, together with some pion events in which both pions pass the calorimeter without nuclear interaction.

Separation of pion and muon events in the CsI calorimeter is illustrated in Fig. 1, where scatter plots of the energy deposition of one track vs. that of the other one are presented for events with one or no hits in the muon system (a) and selected as muons (b). Energy depositions are corrected for the incident angle. Pions can have nuclear

interactions and in some cases leave more energy, while muons mostly exhibit dE/dx losses only.

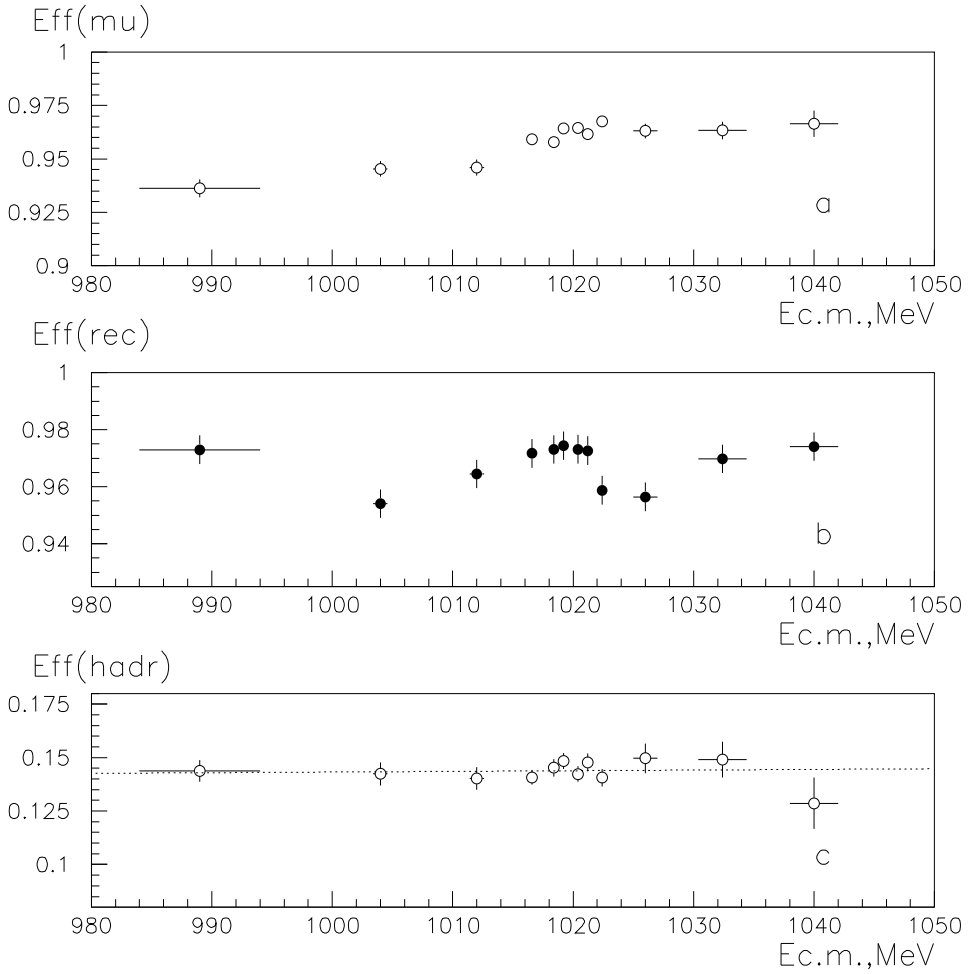

Figure 2: a.Muon system efficiency vs. energy. b.Reconstruction efficiency for DC. c.Probability for two pions to be selected as muons.

To select a cleaner sample of muon events, in addition to the information from the muon system both tracks were required to show only minimum ionizing energy deposition in the calorimeter (60-130 MeV). All the remaining events were considered as pion candidates. In this raw separation the pion sample $N_{\pi\pi\gamma}$ contains muons because of some inefficiency of the muon system while the muon sample $N_{\mu\mu\gamma}$ contains pions since a pion can reach the muon system without nuclear interaction. The observed numbers of events $N_{\pi\pi\gamma}$ and $N_{\mu\mu\gamma}$ are related to the true numbers $N^0_{\pi\pi\gamma}$ and $N^0_{\mu\mu\gamma}$ as:
$N_{\pi\pi\gamma} = (1-\epsilon_\mu)\cdot N^0_{\mu\mu\gamma} + (1-\epsilon_\pi)\cdot N^0_{\pi\pi\gamma}$,
$N_{\mu\mu\gamma} = \epsilon_\mu \cdot N^0_{\mu\mu\gamma} + \epsilon_\pi \cdot N^0_{\pi\pi\gamma}$,
where ϵ_μ and ϵ_π are the muon system efficiency and probability for a pion pair to be selected as muons respectively.

The magnitudes of ϵ_μ and ϵ_π were determined by studying correlations between the

energy deposition in the CsI calorimeter and response of the muon system to collinear $\pi^+\pi^-$ and $\mu^+\mu^-$ events. The results of this study are shown in Fig. 2 for one of the experimental scans. Figure 2a presents the muon system efficiency for different energy points. Only statistical errors are shown. The probability for two pions to be selected as muons is presented in Fig. 2c and is independent of the possible instability of the detection system.

The number of pions and muons has been corrected for the DC reconstruction efficiency shown in Fig. 2b. This efficiency was determined from collinear Bhabha events as described in [9].

Our study of the efficiencies gives a correlated 3% systematic uncertainty in the final number of $\pi^+\pi^-$ and $\mu^+\mu^-$ events.

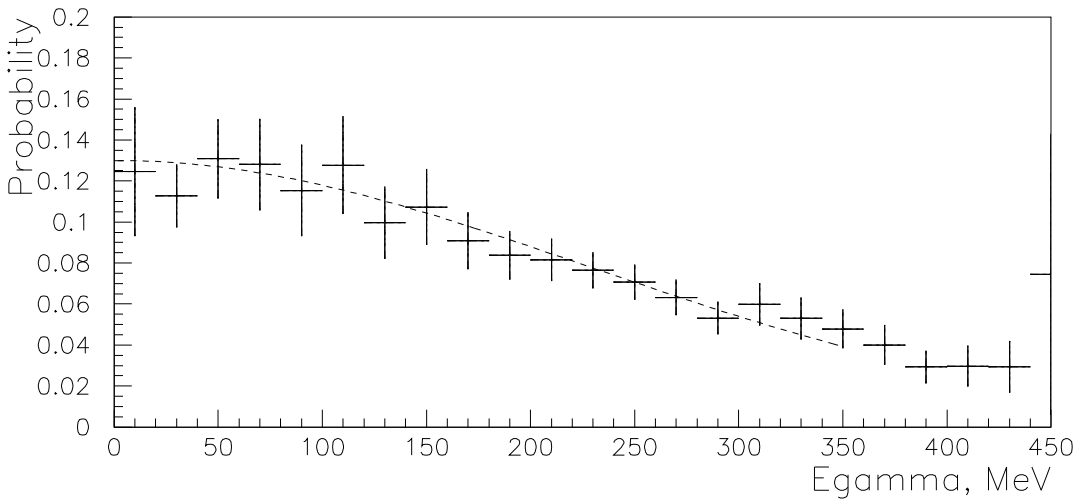

Figure 3: Simulated probability for pions to be selected as muons vs. photon energy.

For events with photons ϵ_μ and ϵ_π depend on photon energy. This dependence was studied using simulated $\pi^+\pi^-\gamma$ events. The probability of two pions to be selected as muons varies with photon energy as presented in Fig. 3 and was used to correct the final number of events with photons. At low photon energy this probability is consistent with that obtained from collinear events (see Fig. 2c).

Constrained Fit

To reduce the background from collinear events as well as that from the three pion ϕ decay a constrained fit was used requiring total energy-momentum conservation for a three body decay. About 20% of the selected events had an additional photon. In this case the constrained fit was applied to both possible combinations and that with a minimum χ^2 was chosen.

An additional cut was applied to the photon direction: an azimuthal angle should be more than 0.25 radians from the charged track direction. This cut removed the remaining collinear events with a background photon which survived after the constrained fit.

The χ^2/d.f. distribution for events selected as muons had very small background and was found to be in good agreement with simulation as shown in Fig. 4a. Motivated

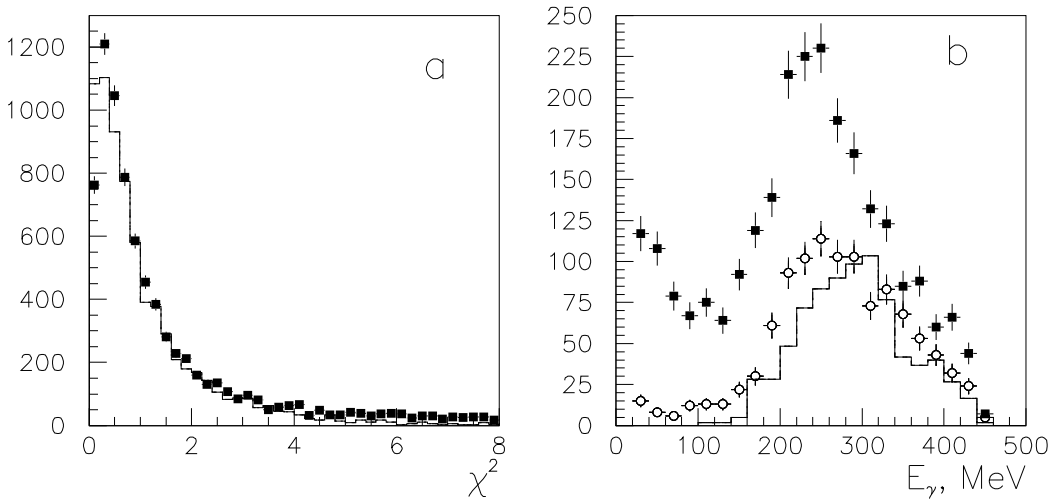

Figure 4: a. The χ^2/d.f. distribution for events selected as muons. The histogram is simulation. b. Photon spectrum for events selected as pions for χ^2/d.f.<3 (dark points) and for $3 < \chi^2/\text{d.f.} < 6$ (open points). The histogram is simulation of background from $\pi^+\pi^-\pi^0$ events.

by simulation, a cut that χ^2/d.f. be less than 3 was imposed for pion and muon events selecting 95% of signal events.

After the above cut the pion sample still contained some background mainly from three pion ϕ decays. Such three pion background appears when one of the photons from the π^0 has energy below 20 MeV and is not detected so that the event looks like a three body decay with the remaining photon energy higher than 150 MeV. The χ^2/d.f distribution for these events was flat and events with $3 < \chi^2/\text{d.f.} < 6$, shown in Fig. 4b by open points, were used to estimate the background spectrum. At each energy the background spectrum was subtracted from that for the signal candidates.

From a constrained fit one can obtain an improved estimate for the photon energy. This effect was studied by using simulation and results are presented in Fig. 5. Simulation shows that after the constrained fit photons have energy resolution about 5 MeV in the whole energy range instead of $\sigma_{E_\gamma} = 8\% \times E_\gamma$ CsI resolution as shown in Figs. 5a,b. Figure 5c demonstrates the simulated photon detection efficiency in the

CsI calorimeter vs. photon energy. The overall detector efficiency vs. photon energy is shown in Fig. 5d for $\pi^+\pi^-\gamma$ events.

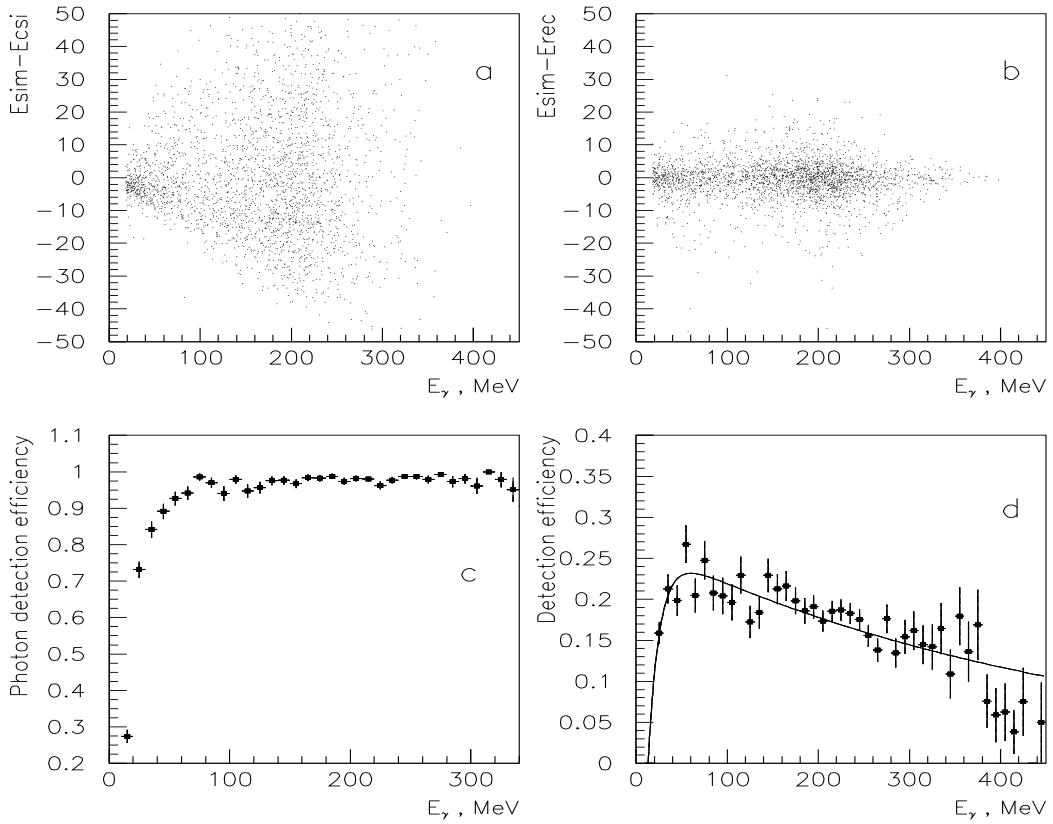

Figure 5: Study of simulated $\pi^+\pi^-\gamma$ events. a. Difference between the photon energy measured in the calorimeter and the initially simulated one vs. photon energy. b. Difference between the kinematically reconstructed photon energy and the initially simulated one vs. photon energy. c. Simulated photon detection efficiency in the CsI calorimeter. d. Overall detector efficiency vs. photon energy.

To extract the resonant contribution associated with the ϕ, two data sets were used. The first set ("ϕ" region) for $E_{c.m.}$ from 1016.0 to 1023.2 MeV had the integrated luminosity of 9.24 pb^{-1} while the second one ("off-ϕ" region) taken at $E_{c.m.}$ = 996-1013 and 1026-1060 MeV with the integrated luminosity of 3.89 pb^{-1} containing less than 3% ϕ decays was used for a background estimate.

Figure 6 presents photon spectra obtained after background subtraction and corrections for the detector efficiency at the "ϕ" (a,c) and "off-ϕ" (b,d) regions for pions and muons respectively. The solid line corresponds to the theoretical calculation [11] taking into account the integrated luminosity at each energy point and $\rho-\omega$ mixing for the bremsstrahlung process. A peak at 220 MeV is due to the radiation by initial electrons resulting in the process $e^+e^- \to \rho\gamma$, $\rho \to \pi^+\pi^-$. The photon energy range

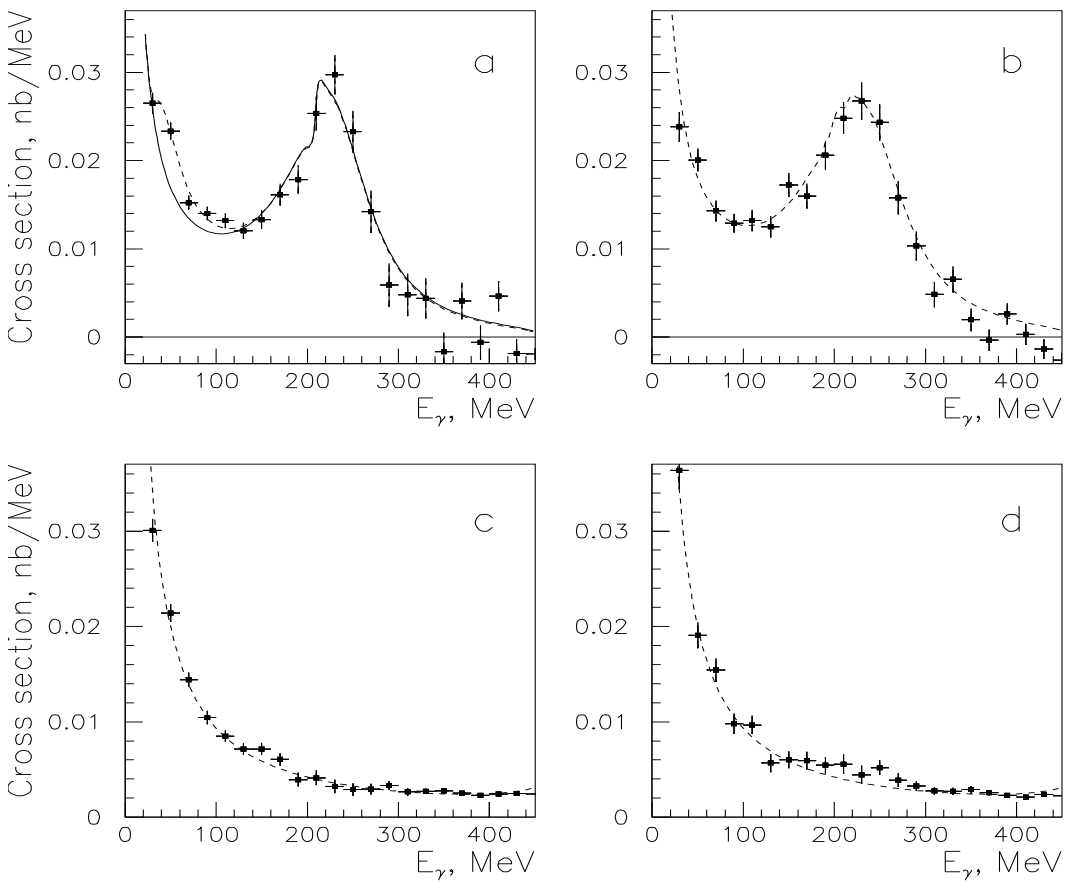

Figure 6: a. Photon spectrum for $\pi^+\pi^-\gamma$ events at the "ϕ" region; Solid line is pure bremsstrahlung. Dashed lines include a possible ϕ signal according to [11]. b. Photon spectrum for $\pi^+\pi^-\gamma$ events at the "off-ϕ" region; c,d. The same spectra for $\mu^+\mu^-\gamma$ events.

20 to 120 MeV has minimum background and some excess of events over the expected bremsstrahlung spectrum (the solid line in Fig. 6a) can be seen in the $\pi^+\pi^-\gamma$ sample at the "ϕ" region. In total, 30175 $\pi^+\pi^-\gamma$ events and 27188 $\mu^+\mu^-\gamma$ events have been selected in this energy range.

Cross Section Study

The cross section for each energy point was calculated as $\sigma = N_{ev}/(\mathrm{L}\cdot\epsilon)$. N_{ev} is the number of selected events with photons in the energy range from 20 to 120 MeV. The integrated luminosity L for each energy point was determined from Bhabha events with about 2% systematic accuracy [9]. The detection efficiency ϵ was obtained by simulation and the approximation shown by the solid line in Fig. 5d was used to correct photon spectra.

The resulting cross sections of the processes $e^+e^- \to \pi^+\pi^-\gamma$ and $e^+e^- \to \mu^+\mu^-\gamma$

versus energy are presented in Fig. 7a,b. Only statistical errors are shown. The systematic error in the experimental cross sections was estimated to be about 5% dominated by the uncertainty of the pion-muon separation efficiencies.

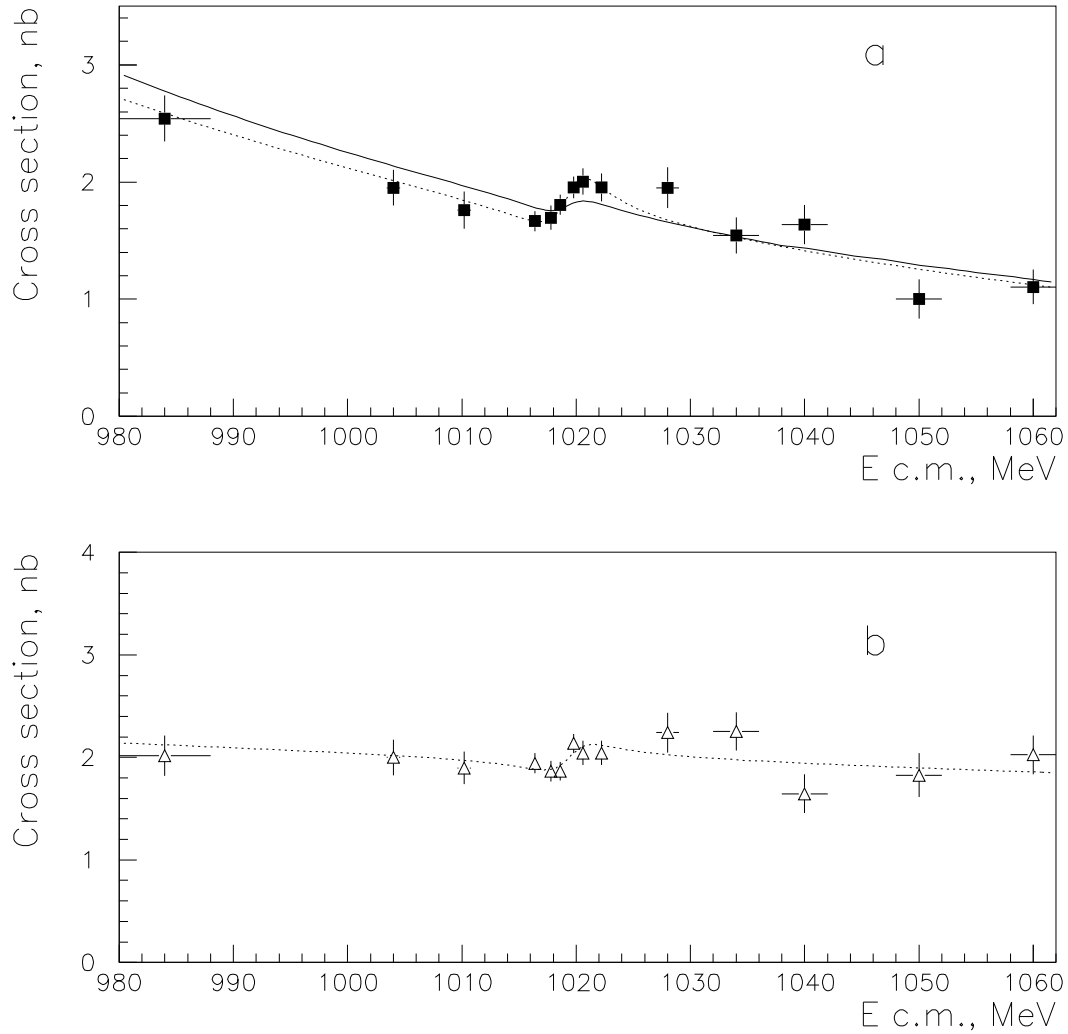

Figure 7: a. Cross section for $e^+e^- \to \pi^+\pi^-\gamma$. Lines are theoretical predictions in case of no direct ϕ decay (solid line) and best fit (dotted line). b. Cross section for $e^+e^- \to \mu^+\mu^-\gamma$ with the theoretical prediction.

The cross sections can be described according to the calculations performed in [2, 11]. It has been shown there that the amplitudes describing initial bremsstrahlung differ from those for the final bremsstrahlung and the ϕ meson, so that the differential cross section for $\pi^+\pi^-\gamma$ events is:

$$\frac{d\sigma(s,E_\gamma)}{dE_\gamma} \approx |A^{in}_{br}(s,E_\gamma)|^2 + |A^{f}_{br}(s,E_\gamma) + A_\phi(s,E_\gamma) \pm e^{i\Psi}\cdot A_{f_0}(s,E_\gamma)|^2.$$

Here $A^{in}_{br}(s,E_\gamma)$ and $A^{in}_{br}(s,E_\gamma)$ are the amplitudes describing initial and final bremsstrahlung processes, and the amplitude $A_\phi(s,E_\gamma)$ introduces the influence of the ϕ upon the

photon propagator (a vacuum polarization term). This contribution gives rise to an interference pattern in the cross section at the ϕ mass and can be referred to as an "electromagnetic" decay $\phi \to \gamma \to \pi^+\pi^-\gamma$ or $\phi \to \gamma \to \mu^+\mu^-\gamma$. The amplitude of the interference is determined by the ϕ meson leptonic coupling constant.

The amplitude $A_{f_0}(s, E_\gamma)$ represents the possible ϕ decay into the $\pi^+\pi^-\gamma$ final state via $f_0\gamma$. For $\mu^+\mu^-\gamma$ events $A_{f_0}(s, E_\gamma) = 0$. The model considers the f_0 meson as a two- or four-quark state or $K\bar{K}$ molecule depending on the values of the coupling constants $g^2_{K\bar{K}}/4\pi$ and $g^2_{\pi\pi}/4\pi$.

It also includes the interference of the ϕ amplitude with the final bremsstrahlung amplitude $A^f_{br}(s, E_\gamma)$ as well as the correction for the $\pi^+\pi^-$ scattering in the final state [13]. The latter effect gives a contribution of about 15% to the branching ratio, but within our accuracy can be introduced as an additional phase shift Ψ between the amplitudes of the ϕ and bremsstrahlung process. This shift was predicted to be 1.2-1.4 radians, but the sign of the term was unknown and was determined from the fit. In general, all amplitudes have different dependence on s and E_γ.

The initial bremsstrahlung process presented by the amplitude $A^{in}_{br}(s, E_\gamma)$ is suppressed by selecting photons transverse to the beam direction, but it still accounts for about 2/3 [11] of the observed $e^+e^- \to \pi^+\pi^-\gamma$ and one half of the $e^+e^- \to \mu^+\mu^-\gamma$ cross section.

Integration over E_γ from 20 to 120 MeV gives $\sigma(s)$ which can be used for the cross section aproximation in Fig. 7.

Assuming no hadronic $\phi \to \pi^+\pi^-\gamma$ decay ($A_{f_0}(s, E_\gamma)$=0) a simple formula has been used where the final radiation amplitude of the bremsstrahlung process interferes with the Breit-Wigner amplitude from the ϕ vacuum polarization:

$$\sigma(s) = \sigma^{in}_{br}(s) + \sigma^f_{br}(s) \cdot |1 - e^{i\psi} \cdot A^{(0)}_\phi \frac{m_\phi \Gamma_\phi}{\Delta_\phi}|^2;$$

$$\Delta_\phi = s - m^2_\phi + i\sqrt{s}\Gamma_\phi(s).$$

Here $s = 4E^2_{beam}$, Γ_ϕ and m_ϕ are ϕ meson parameters, $A^{(0)}_\phi$ is the ϕ decay amplitude in the peak and ψ is the relative phase between the bremsstrahlung and ϕ decay amplitudes.

This formula is valid under the natural assumption of the same photon spectrum for the final radiation amplitude of the bremsstrahlung process and the Breit-Wigner amplitude of the "electromagnetic" ϕ decay.

The initial $\sigma^{in}_{br}(s)$ and final $\sigma^f_{br}(s)$ bremsstrahlung cross sections have different energy dependence for 20-120 MeV photons because of the pion formfactor energy behaviour. According to [11] the power functions $\sigma^{in}_{br}(s) = 0.65 \cdot \sigma_0 \cdot (m_\phi/\sqrt{s})^{13}$

and $\sigma_{br}^{f}(s) = 0.35 \cdot \sigma_0 \cdot (m_\phi/\sqrt{s})^9$ can describe the bremsstrahlung process $e^+e^- \to \pi^+\pi^-\gamma$ in our energy range. The parameter σ_0 represents the sum of initial and final bremsstrahlung cross section at the ϕ mass. The function $\sigma_{br}^{in}(s) = \sigma_{br}^{f}(s) = 0.5 \cdot \sigma_0(m_\phi^2/s)$ was used for muons.

The fit of experimental data with σ_0, peak amplitude $A_\phi^{(0)}$ and ψ as free parameters shows good agreement of obtained cross sections with the theoretical calculations [11]:
$\sigma_0^{exp}/\sigma_0^{th} = 1.02 \pm 0.02 \pm 0.05$,
$\sigma_0^{exp}/\sigma_0^{th} = 0.97 \pm 0.02 \pm 0.05$
for pions and muons respectively. The above values also indicate that the $\mu - \pi$ separation uncertainty does not exceed the estimated systematic error.

Using the obtained amplitude one can calculate the peak cross section $\sigma(\phi \to \pi\pi\gamma) = |A_\phi^{(0)}|^2 \cdot \sigma_{br}^{f}(m_\phi^2)$ and the decay branching ratio can be calculated as $Br(\phi \to \pi\pi\gamma) = \sigma(\phi \to \pi\pi\gamma)/\sigma_{tot}^{\phi}$, where σ_{tot}^{ϕ} is the total peak cross section of the ϕ resonance obtained from the leptonic width [1]. The following results have been obtained after inserting corrections for angular acceptance equal to 0.68 and 0.42 for pions and muons respectively:

$Br(\phi \to \pi^+\pi^-\gamma) = (0.41 \pm 0.12 \pm 0.04) \times 10^{-4}$,

$Br(\phi \to \mu^+\mu^-\gamma) = (1.43 \pm 0.45 \pm 0.14) \times 10^{-5}$,

$\psi = (0.46 \pm 0.17)$ radians for pions and $\psi = (0.2 \pm 0.4)$ radians for muons.

The obtained values should be compared to the theoretical calculations based on "electromagnetic" ϕ decays only [11]:

$Br(\phi \to \pi^+\pi^-\gamma)$=$0.047 \times 10^{-4}$,

$Br(\phi \to \mu^+\mu^-\gamma)$=$1.15 \times 10^{-5}$.

For muons the experimental value is in good agreement with theory, but for pions the value of the measured branching ratio is 9 times larger than the theoretical expectation and points to the presence of the hadronic decay of ϕ to $\pi^+\pi^-\gamma$. The obtained branching ratios supersede our results in [5] based on the part of the total data sample. The corresponding fit curves are shown in Fig. 7.

Studies of Photon Spectra

To search for the $\phi \to f_0(980)\gamma$ decay contribution to the observed $\phi \to \pi^+\pi^-\gamma$ decay, photon energy spectra were studied. The photon spectra from the "ϕ" region are shown in Fig. 8 for six c.m.energy points and photons in the 20-160 MeV energy range. The spectra were corrected for all experimental inefficiencies and normalized to the integrated luminosity.

The signal from the decay of the $\phi \to f_0(980)\gamma$ is seen as a structure in the photon spectra at 40-60 MeV. Also shown by the dotted lines are the theoretical predictions

for the expected bremsstrahlung spectra [11, 13] including vacuum polarization .

Because of the presence of the resonance in the photon spectra the branching ratio obtained in the previous chapter for the $\phi \to \pi^+\pi^-\gamma$ decay can be used only as some indication to the existence of the ϕ hadronic decay into this mode.

It should be mentioned that the excess of events over the bremsstrahlung spectra cannot be used for the branching ratio calculation. As it was shown in [8, 5, 11], the destructive interference with the bremsstrahlung process can reduce a visible signal in the selected energy range for photons. To demonstrate the effect of interference the

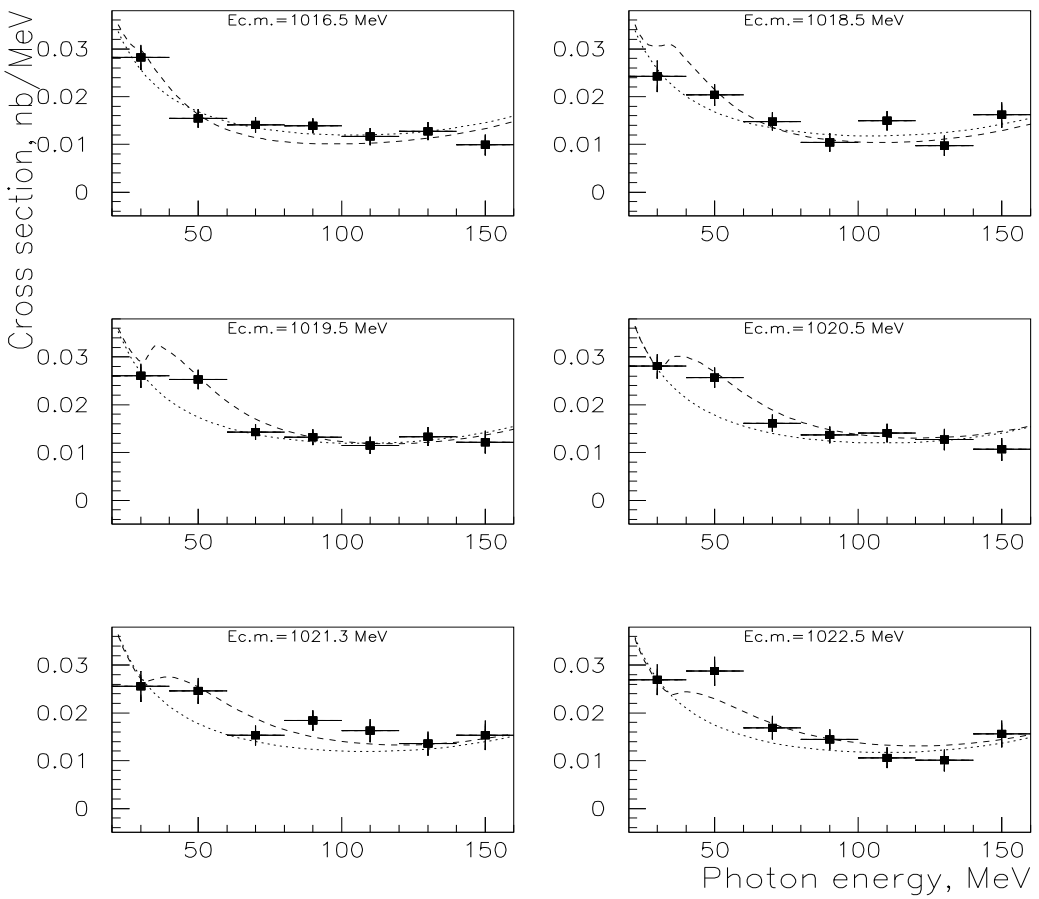

Figure 8: Photon spectra for six c.m.energy points in the "ϕ" region. Lines are theoretical predictions for the four quark model (dashed line) and pure bremsstrahlung spectra (dotted line).

photon spectra in Fig. 8 were fit as a group with the spectra calculated for each energy point using the differential cross section from [2, 11] (see previous section).

The number of events was not sufficient to keep all model parameters free and therefore the model parameters $g^2_{K\bar{K}}/4\pi$ and $g^2_{\pi\pi}/4\pi$ were varied to keep the $f_0(980)$ width at about 40 MeV [1]. The fit had the following free parameters: the branching

ratio, $f_0(980)$ mass and phase shift Ψ. The data can be described by the model only for the destructive interference between the f_0 amplitude and the bremsstrahlung process. The following results have been obtained:

$Br(\phi \to f_0(980)\gamma) = (1.93 \pm 0.46 \pm 0.50) \times 10^{-4}$;

$m_{f_0} = 976 \pm 5 \pm 6$ MeV;

$\Psi = 1.55 \pm 0.22$ radians.

The results above include a systematic error from the weak dependence on the $f_0(980)$ width. The relatively large value of the branching ratio obtained in the fit can not be accounted for by the models assuming the normal $q\bar{q}$ structure of $f_0(980)$ [14] and is predicted only in case of its four quark structure. Note also that it significantly differs from the branching ratio obtained from the simple fit assuming the same photon spectra for all processes.

Search for $\phi \to \rho\gamma$ Decay

The selected $\pi^+\pi^-\gamma$ events with photon energies from 100 to 300 Mev (see Fig. 6) can be used to search for the C-violating decay $\phi \to \rho\gamma$, $\rho \to \pi^+\pi^-$. The cross section vs. energy for the events with photons in the 100-300 MeV range is presented in Fig. 9. The final state in the C-violating $\phi \to \rho\gamma$ decay has the same quantum numbers

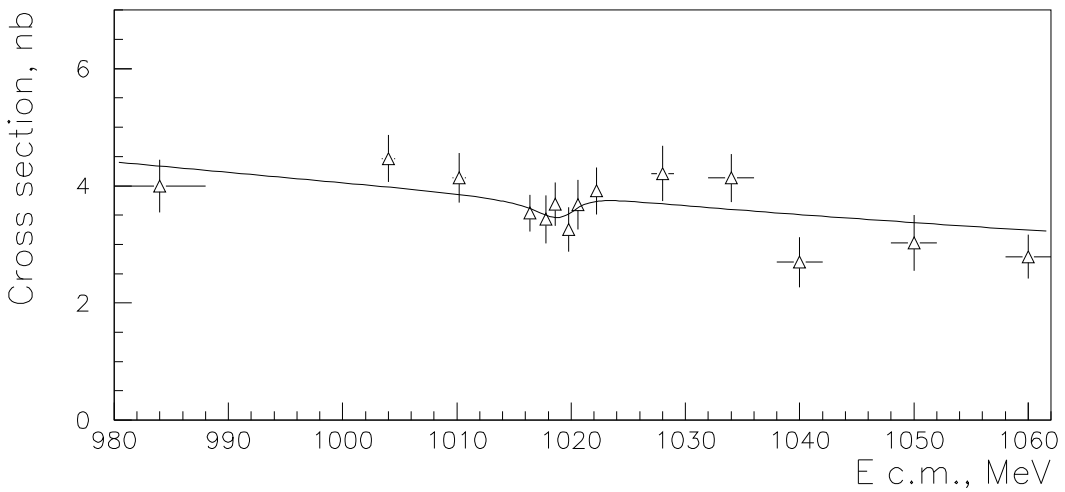

Figure 9: $\phi \to \rho\gamma$ search. The cross section for $\pi^+\pi^-\gamma$ events with photons in the 100-300 MeV range. The line is the best fit.

as in the initial bremsstrahlung process which dominates in the cross section and to extract a possible signal the interference of these two processes is assumed:

$$\sigma(s) = \sigma_{br}^{in}(s) \cdot |1 - e^{i\psi} \cdot \sqrt{\frac{\sigma(\phi\to\rho\gamma)}{\sigma_{br}^{in}(s)}} \cdot \frac{m_\phi \Gamma_\phi}{\Delta_\phi}|^2,$$

where $\sigma_{br}^{in}(s) = \sigma_0 \cdot m_\phi^2/s$. The comparison of the obtained cross section with the theoretical calculation [11] gives the ratio $\sigma_0^{exp}/\sigma_0^{th}$=1.04±0.03. As a result of the fit, $Br(\phi \to \rho\gamma) = \sigma(\phi \to \rho\gamma)/\sigma_{tot}^{\phi} = (0.3 \pm 0.5) \times 10^{-5}$ and $\psi = -0.9 \pm 1.0$ radians have been obtained. Taking into account the 80% detection efficiency, the corresponding upper limit is: $Br(\phi \to \rho\gamma) < 1.2 \times 10^{-5}$ at 90% C.L.

This result should be compared to the previous measurements which gave upper limits 7×10^{-4} [5] and 2×10^{-2} [15].

Search for $\eta \to \pi^+\pi^-$ Decay

The selected $\pi^+\pi^-\gamma$ events can be used to search for the P- and CP- violating decay $\eta \to \pi^+\pi^-$, where the η comes from the radiative $\phi \to \eta\gamma$ decay. From 19.7 millions of ϕ decays used for the $\pi^+\pi^-\gamma$ channel analysis one could expect about 248,000 events which decayed via the $\eta\gamma$ channel. These P-, CP-violating decays should be observed as peaks in the invariant mass of two pions at $m_{\pi\pi} = m_\eta$. Figure 10

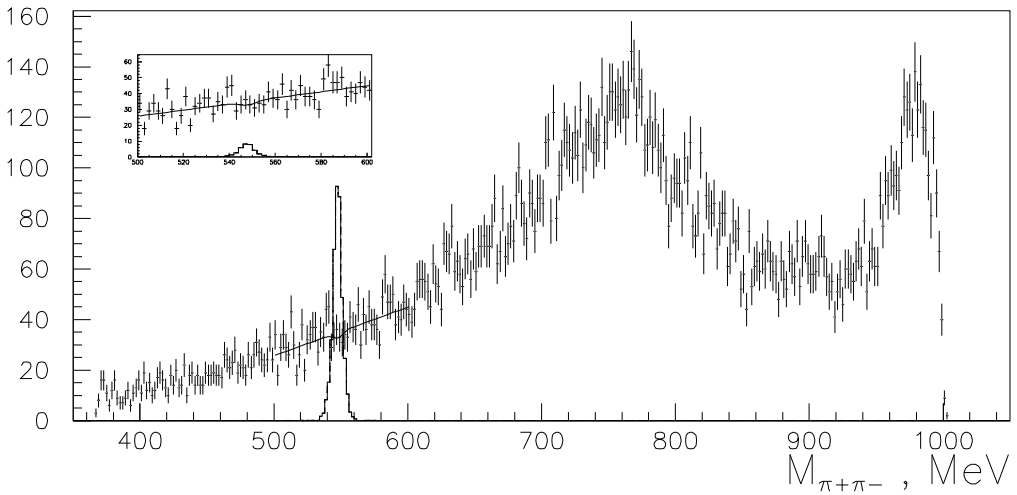

Figure 10: Search for $\eta \to \pi^+\pi^-$ decay. The histogram in the box shows a simulated possible signal at 90% CL.

represents experimental distributions of $\pi^+\pi^-$ masses from selected $\pi^+\pi^-\gamma$ events. The line corresponds to a fit with a linear function and gaussian distribution representing a possible signal. It was found that the signal does not exceed 10 events at 90% CL. The histogram in the box shows a simulated signal from $\eta \to \pi^+\pi^-$ decays at 90% CL. The detection efficiency found by simulation was 0.124. The following result has been obtained:

$\mathrm{Br}(\eta \to \pi^+\pi^-) < 3.3 \times 10^{-4}$.
which should be compared to the best previous limit of 9×10^{-4} [5].

Conclusions

Using 13.1 pb^{-1} of data collected around the ϕ meson (about 20 millions of the ϕ decays) $e^+e^- \to \pi^+\pi^-\gamma$ and $e^+e^- \to \mu^+\mu^-\gamma$ events were selected. For the first time the decay $\phi \to \pi^+\pi^-\gamma$ has been observed in the 20-120 MeV photon energy range. The fit assuming that the ϕ contributes only to the photon propagator (no direct ϕ decay) gave the branching ratio:

$Br(\phi \to \pi^+\pi^-\gamma) = (0.41 \pm 0.12 \pm 0.04) \times 10^{-4}$.

This value is nine times higher than the expected and points to the presence of the hadronic decay of the ϕ into this final state. The analysis of the photon spectra shows the presence of a resonance in the $\pi^+\pi^-$ system with a mass of about 980 MeV. The obtained branching ratio can be affected by the complicated interference of the hadronic ϕ decay with the bremsstrahlung process. The effect of interference was demonstrated by fitting photon spectra assuming the $\phi \to f_0(980)\gamma$ decay and the following results have been obtained:

$Br(\phi \to f_0(980)\gamma) = (1.93 \pm 0.46 \pm 0.50) \times 10^{-4}$;

$m_{f_0} = 976 \pm 5 \pm 6$ MeV;

$\Psi = 1.55 \pm 0.22$ radians,

where Ψ is the relative phase of the amplitudes of the ϕ decay and the bremsstrahlung process taking into account the final state $\pi - \pi$ interaction.

According to the model [2, 11, 13], the obtained branching ratio can only be explained if $f_0(980)$ is a four quark state.

For muons the value

$Br(\phi \to \mu^+\mu^-\gamma) = (1.43 \pm 0.45 \pm 0.14) \times 10^{-5}$

has been obtained for the photon energies $E_\gamma > 20MeV$ consistent with the theoretical expectations.

For the C-violating decay of $\phi \to \rho\gamma$ and P-, CP-violating decay of $\eta \to \pi^+\pi^-$ the following upper limits at 90% CL have been obtained:

$Br(\phi \to \rho\gamma) \ < \ 1.2 \times 10^{-5}$,

$Br(\eta \to \pi^+\pi^-) \ < \ 3.3 \times 10^{-4}$.

These results are the most stringent upper limits at the moment [1].

Analysis of the $f_0(980)\gamma$ intermediate state is continued in the following paper devoted to the studies of the $\pi^0\pi^0\gamma$ and $\eta\pi^0\gamma$ final states [16].

Acknowledgements

The authors are grateful to N.N.Achasov, V.P.Druzhinin, V.V.Gubin, V.N.Ivanchenko and A.I.Milstein for useful discussions and help with the data interpretation.

REFERENCES

1. C.Caso *et al.*, Eur.Phys.J. **C3** (1998) 1, Review of Particle Physics.
2. N.N.Achasov and V.N.Ivanchenko, Nucl. Phys. **B315** (1989) 465.
3. F.E. Close, N. Isgur and S. Kumano, Nucl. Phys. **B389** (1993) 513.
4. S.I.Dolinsky *et al.*, Phys. Rep. **202** (1991) 99.
5. R.R. Akhmetshin *et al.*, Phys. Lett. **B415** (1997) 452.
6. M.N.Achasov *et al.*, Phys. Lett. **B438** (1998) 441.
7. M.N.Achasov *et al.*, Phys. Lett. **B440** (1998) 442.
8. E.Solodov (CMD-2 collaboration), Proc. of the 29th Conf. on High Energy Phys. 19-24 July.1998, Vancouver, Canada.
9. R.R.Akhmetshin *et al.*, Preprint BudkerINP 99-11, Novosibirsk, 1999.
10. V.V.Anashin *et al.*, Preprint INP 84-114, Novosibirsk, 1984.
11. N.N.Achasov, V.V.Gubin and E.P.Solodov, Phys. Rev. **D55** (1997) 2672.
12. G.A.Aksenov *et al.*, Preprint BudkerINP 85-118, Novosibirsk, 1985.
    E.V. Anashkin *et al.*, ICFA Instrumentation Bulletin **5** (1988) 18.
13. N.N.Achasov and V.Gubin, Phys. Rev. **D57** (1998) 1987.
14. S.Nussinov and Tran N. Truong, Phys. Rev. Lett. **63** (1989) 1349.
    A.A. Pivovarov, Soviet Physics - Lebedev Institute Reports **9** (1990) 12.
    N. Paver, contribution to the ϕ Factory Workshop at UCLA, April, 1990.
    J.L. Lucio and J.Pestieau, Phys. Rev. **D42** (1990) 3253.
    S. Fajfer and R.J. Oakes, Phys. Rev. **D42** (1990) 2392.
15. J.S.Lindsey *et al.*, Phys. Rev. **147** (1966) 913.
16. R.R.Akhmetshin *et al.*, the following paper.